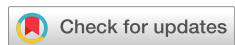


PAPERS | JUNE 01 2015

## Visualizing *Interstellar's* Wormhole

Oliver James; Eugénie von Tunzelmann; Paul Franklin; Kip S. Thorne



*Am. J. Phys.* 83, 486–499 (2015)

<https://doi.org/10.1119/1.4916949>



View  
Online



Export  
Citation

### Articles You May Be Interested In

Geodesy on surfaces of revolution: A wormhole application

*Am. J. Phys.* (April 2020)

Embeddings and time evolution of the Schwarzschild wormhole

*Am. J. Phys.* (March 2012)

Empirical exploration of timelike geodesics around a rotating wormhole

*Am. J. Phys.* (May 2016)

# Visualizing *Interstellar's* Wormhole

Oliver James, Eugénie von Tunzelmann, and Paul Franklin

*Double Negative Ltd, 160 Great Portland Street, London W1W 5QA, United Kingdom*

Kip S. Thorne

*California Institute of Technology, Pasadena, California 91125*

(Received 27 November 2014; accepted 24 March 2015)

Christopher Nolan's science fiction movie *Interstellar* offers a variety of opportunities for students in elementary courses on general relativity theory. This paper describes such opportunities, including: (i) At the motivational level, the manner in which elementary relativity concepts underlie the wormhole visualizations seen in the movie; (ii) At the briefest computational level, instructive calculations with simple but intriguing wormhole metrics, including, e.g., constructing embedding diagrams for the three-parameter wormhole that was used by our visual effects team and Christopher Nolan in scoping out possible wormhole geometries for the movie; (iii) Combining the proper reference frame of a camera with solutions of the geodesic equation, to construct a light-ray-tracing map backward in time from a camera's local sky to a wormhole's two celestial spheres; (iv) Implementing this map, for example, in Mathematica, Maple or Matlab, and using that implementation to construct images of what a camera sees when near or inside a wormhole; (v) With the student's implementation, exploring how the wormhole's three parameters influence what the camera sees—which is precisely how Christopher Nolan, using our implementation, chose the parameters for *Interstellar's* wormhole; (vi) Using the student's implementation, exploring the wormhole's Einstein ring and particularly the peculiar motions of star images near the ring, and exploring what it looks like to travel through a wormhole. © 2015 Author(s). All article content, except where otherwise noted, is licensed under a Creative Commons Attribution 3.0 Unported License.

[<http://dx.doi.org/10.1119/1.4916949>]

## I. INTRODUCTION

### A. The context and purposes of this paper

In 1988, in connection with Carl Sagan's novel *Contact*,<sup>1</sup> later made into a movie,<sup>2</sup> one of the authors published an article in this journal about wormholes as a tool for teaching general relativity.<sup>3</sup>

This article is a follow-up, a quarter century later, in the context of Christopher Nolan's movie *Interstellar*<sup>4</sup> and Kip Thorne's associated book *The Science of Interstellar*.<sup>5</sup> Like *Contact*, *Interstellar* has real science built into its fabric, thanks to a strong science commitment by the director, screenwriters, producers, and visual effects team, and thanks to Thorne's role as an executive producer.

Although wormholes were central to the theme of *Contact* and to many movies and TV shows since then, including *Star Trek* and *Stargate*, none of these have depicted correctly a wormhole as it would be seen by a nearby human. *Interstellar* is the first to do so. The authors of this paper, together with Christopher Nolan who made key decisions, were responsible for that depiction.

This paper has two purposes: (i) To explain how *Interstellar's* wormhole images were constructed and explain the decisions made on the way to their final form and (ii) to present this explanation in a way that may be useful to students and teachers in elementary courses on general relativity.

### B. The status of wormholes in the real universe

Before embarking on these explanations, we briefly describe physicists' current understanding of wormholes based on much research done since 1988. For a thorough and

readable, but non-technical review, see the recent book *Time Travel and Warp Drives* by Allen Everett and Thomas Roman.<sup>6</sup> For reviews that are more technical, see papers by Friedman and Higuchi<sup>7</sup> and by Lobo.<sup>8</sup>

In brief, physicists' current understanding is this:

- There is no known mechanism for making wormholes, either naturally in our universe or artificially by a highly advanced civilization, but there are speculations; for example, that wormholes in hypothetical quantum foam on the Planck scale,  $\sqrt{G\hbar/c^3} \sim 10^{-35}$  m, might somehow be enlarged to macroscopic size.<sup>6,9</sup>
- Any creation of a wormhole where initially there is none would require a change in the topology of space, which would entail, in classical, non-quantum physics, both negative energy and closed timelike curves (the possibility of backward time travel)—according to theorems by Frank Tipler and Robert Geroch.<sup>7</sup> It is likely the laws of physics forbid this. Likely, but not certain.
- A wormhole will pinch off so quickly that nothing can travel through it, unless it has “exotic matter” at its throat—matter (or fields) that, at least in some reference frames, has negative energy density. Although such negative energy density is permitted by the laws of physics (e.g., in the Casimir effect, the electromagnetic field between two highly conducting plates), there are quantum inequalities that limit the amount of negative energy that can be collected in a small region of space and how long it can be there; and these appear to place severe limits on the sizes of traversable wormholes (wormholes through which things can travel at the speed of light or slower).<sup>6</sup> The implications of these inequalities are not yet fully clear, but it seems likely that, after some strengthening, they will prevent macroscopic wormholes like the one in *Interstellar* from



staying open long enough for a spaceship to travel through. Likely, but not certain.

- The research leading to these conclusions has been performed ignoring the possibility that our universe, with its four spacetime dimensions, resides in a higher dimensional *bulk* with one or more large extra dimensions, the kind of bulk envisioned in *Interstellar*'s "fifth dimension." Only a little is known about how such a bulk might influence the existence of traversable wormholes, but one intriguing thing is clear: Properties of the bulk can, at least in principle, hold a wormhole open without any need for exotic matter in our four dimensional universe (our "brane").<sup>8</sup> But the words "in principle" just hide our great ignorance about our universe in higher dimensions.

In view of this current understanding, it seems very unlikely to us that traversable wormholes exist naturally in our universe, and the prospects for highly advanced civilizations to make them artificially are also pretty dim.

Nevertheless, the distances from our solar system to others are so huge that there is little hope, using rocket technology, for humans to travel to other stars in the next century or two;<sup>10</sup> so wormholes, quite naturally, have become a staple of science fiction.

And, as Thorne envisioned in 1988,<sup>3</sup> wormholes have also become a pedagogical tool in elementary courses on general relativity—e.g., in the textbook by James Hartle.<sup>11</sup>

### C. The genesis of our research on wormholes

This paper is a collaboration between Caltech physicist Kip Thorne, and computer graphics artists at *Double Negative Visual Effects* in London. We came together in May 2013, when Christopher Nolan asked us to collaborate on building, for *Interstellar*, realistic images of a wormhole, and also a fast spinning black hole and its accretion disk, with ultra-high (IMAX) resolution and smoothness. We saw this not only as an opportunity to bring realistic wormholes and black holes into the Hollywood arena but also an opportunity to create images of wormholes and black holes for relativity and astrophysics research.

Elsewhere<sup>12</sup> we describe the simulation code that we wrote for this project—DNGR for "Double Negative Gravitational Renderer"—and the black-hole and accretion-disk images we generated with it, and also some new insights into gravitational lensing by black holes that it has revealed. In this paper, we focus on wormholes, which are much easier to model mathematically than *Interstellar*'s fast spinning black hole, and are far more easily incorporated into elementary courses on general relativity.

In our modelling of *Interstellar*'s wormhole, we pretended we were engineers in some arbitrarily advanced civilization, and that the laws of physics place no constraints on the wormhole geometries our construction crews can build. (This is almost certainly false; the quantum inequalities mentioned above, or other physical laws, likely place strong constraints on wormhole geometries, if wormholes are allowed at all—but we know so little about those constraints that we chose to ignore them.) In this spirit, we wrote down the spacetime metrics for candidate wormholes for the movie, and then proceeded to visualize them.

### D. Overview of this paper

We begin in Sec. II by presenting the spacetime metrics for several wormholes and visualizing them with embedding diagrams. These metrics include, most importantly, the three-parameter "Dneg wormhole" metric used in our work on the movie *Interstellar*. Then we discuss adding a Newtonian-type gravitational potential to our Dneg metric, to produce the gravitational pull that Christopher Nolan wanted, and the potential's unimportance for making wormhole images.

In Sec. III, we describe how light rays, traveling backward in time from a camera to the wormhole's two celestial spheres, generate a map that can be used to produce images of the wormhole and of objects seen through or around it; and we discuss our implementations of that map to make the images seen in *Interstellar*. In the Appendix, we present a fairly simple computational procedure by which students can generate their own map and thence their own images.

In Sec. IV, we use our own implementation of the map to describe the influence of the Dneg wormhole's three parameters on what the camera sees. Then, in Secs. V and VI, we discuss Christopher Nolan's use of these kinds of implementations to choose the parameter values for *Interstellar*'s wormhole; we discuss the resulting wormhole images that appear in *Interstellar*, including that wormhole's Einstein ring, which can be explored by watching the movie or its trailers, or in students' own implementations of the ray-tracing map; and we discuss images made by a camera travelling through the wormhole, that do not appear in the movie. Finally in Sec. VII, we present brief conclusions.

Scattered throughout the paper are suggestions of calculations and projects for students in elementary courses on general relativity. And throughout, as is common in relativity, we use "geometrized units" in which Newton's gravitational constant  $G$  and the speed of light  $c$  are set equal to unity, so time is measured in length units:  $1\text{ s} = c \times 1\text{ s} = 2.998 \times 10^8\text{ m}$ ; and mass is expressed in length units:  $1\text{ kg} = (G/c^2) \times 1\text{ kg} = 0.742 \times 10^{-27}\text{ m}$ ; and the mass of the Sun is 1.476 km.

## II. SPACETIME METRICS FOR WORMHOLES AND EMBEDDING DIAGRAMS

In general relativity, the curvature of spacetime can be expressed mathematically in terms of a spacetime metric. In this section, we review a simple example of this: the metric for an *Ellis wormhole*; and then we discuss the metric for the *Double Negative (Dneg) wormhole* that we designed for *Interstellar*.

### A. The Ellis wormhole

In 1973 Homer Ellis<sup>13</sup> introduced the following metric for a hypothetical wormhole, which he called a "drainhole"<sup>14</sup>

$$ds^2 = -dt^2 + d\ell^2 + r^2(d\theta^2 + \sin^2\theta d\phi^2), \quad (1)$$

where  $r$  is a function of the coordinate  $\ell$  given by

$$r(\ell) = \sqrt{\rho^2 + \ell^2}, \quad (2)$$

and  $\rho$  is a constant.

As always in general relativity, one does not need to be told anything about the coordinate system in order to figure

out the spacetime geometry described by the metric; the metric by itself tells us everything. Deducing everything is a good exercise for students. Here is how we do so.

First, in  $-dt^2$  the minus sign tells us that  $t$ , at fixed  $\ell, \theta, \phi$ , increases in a timelike direction; and the absence of any factor multiplying  $-dt^2$  tells us that  $t$  is, in fact, proper time (physical time) measured by somebody at rest in the spatial,  $\{\ell, \theta, \phi\}$ , coordinate system.

Second, the expression  $r^2(d\theta^2 + \sin^2\theta d\phi^2)$  is the familiar metric for the surface of a sphere with circumference  $2\pi r$  and surface area  $4\pi r^2$ , written in spherical polar coordinates  $\{\theta, \phi\}$ , so the Ellis wormhole must be spherically symmetric. As we would in flat space, we shall use the name “radius” for the sphere’s circumference divided by  $2\pi$ , i.e., for  $r$ . For the Ellis wormhole, this radius is  $r = \sqrt{\rho^2 + \ell^2}$ .

Third, from the plus sign in front of  $d\ell^2$  we infer that  $\ell$  is a spatial coordinate; and since there are no cross terms  $d\ell d\theta$  or  $d\ell d\phi$ , the coordinate lines of constant  $\theta$  and  $\phi$ , with increasing  $\ell$ , must be radial lines; and since  $d\ell^2$  has no multiplying coefficient,  $\ell$  must be the proper distance (physical distance) traveled in that radial direction.

Fourth, when  $\ell$  is large and negative, the radii of spheres  $r = \sqrt{\rho^2 + \ell^2}$  is large and approximately equal to  $|\ell|$ . When  $\ell$  increases to zero,  $r$  decreases to its minimum value  $\rho$ . And when  $\ell$  increases onward to a very large (positive) value,  $r$  increases once again, becoming approximately  $|\ell|$ . This tells us that the metric represents a wormhole with throat radius  $\rho$ , connecting two asymptotically flat regions of space,  $\ell \rightarrow -\infty$  and  $\ell \rightarrow +\infty$ .

In Hartle’s textbook,<sup>11</sup> a number of illustrative calculations are carried out using Ellis’s wormhole metric as an example. The most interesting is a computation, in Sec. VII, of what the two-dimensional equatorial surfaces (surfaces with constant  $t$  and  $\theta = \pi/2$ ) look like when embedded in a flat 3-dimensional space, the *embedding space*. Hartle shows that equatorial surfaces have the form shown in Fig. 1—a form familiar from popular accounts of wormholes.

Figure 1 is called an “embedding diagram” for the wormhole. We discuss embedding diagrams further in Sec. II B 3, in the context of our Dneg wormhole.

Thomas Müller and colleagues<sup>15</sup> have visualized an Ellis wormhole in various environments by methods similar to those that we lay out below.

## B. The double negative three-parameter wormhole

The Ellis wormhole was not an appropriate starting point for our *Interstellar* work. Christopher Nolan, the movie’s director, wanted to see how the wormhole’s visual

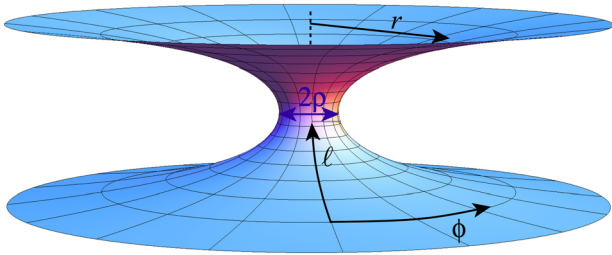


Fig. 1. Embedding diagram for the Ellis wormhole: The wormhole’s two-dimensional equatorial plane embedded in three of the bulk’s four spatial dimensions.

appearance depends on its shape, so the shape had to be adjustable, which is not the case for the Ellis wormhole.

So for *Interstellar* we designed a wormhole with three free shaping parameters and produced images of what a camera orbiting the wormhole would see for various values of the parameters. Christopher Nolan and Paul Franklin, the leader of our Dneg effort, then discussed the images; and based on them, Nolan chose the parameter values for the movie’s wormhole.

In this section, we explain our three-parameter Double Negative (Dneg) wormhole in three steps: First, a variant with just two parameters (the length and radius of the wormhole’s interior) and with sharp transitions from its interior to its exteriors; then a variant with a third parameter, called the *lensing length*, that smooths the transitions; and finally a variant in which we add a gravitational pull.

### 1. Wormhole with sharp transitions

Our wormhole with sharp transitions is a simple cylinder of length  $2a$ , whose cross sections are spheres, all with the same radius  $\rho$ ; this cylinder is joined at its ends onto flat three-dimensional spaces with balls of radius  $\rho$  removed. This wormhole’s embedding diagram is shown in Fig. 2. As always, the embedding diagram has one spatial dimension removed, so the wormhole’s cross sections appear as circles rather than spheres.

Using the same kinds of spherical polar coordinates as for the Ellis wormhole above, the spacetime metric has the general wormhole form (1) with

$$r(\ell) = \begin{cases} \rho & \text{for the wormhole interior, } |\ell| \leq a \\ |\ell| - a + \rho & \text{for the wormhole exterior, } |\ell| > a. \end{cases} \quad (3)$$

### 2. Dneg wormhole without gravity

Our second step is to smooth the transitions between the wormhole interior  $|\ell| < a$  (the cylinder) and the two external universes  $|\ell| > a$ . As we shall see, the smoothed transitions give rise to gravitational lensing (distortions) of the star field behind each wormhole mouth. Such gravitational lensing is a big deal in astrophysics and cosmology these days (see, e.g., the Gravitational Lensing Resource Letter<sup>16</sup>) and, as we discuss in Sec. V C, it shows up in a rather weird way in *Interstellar* near the edges of the wormhole image.

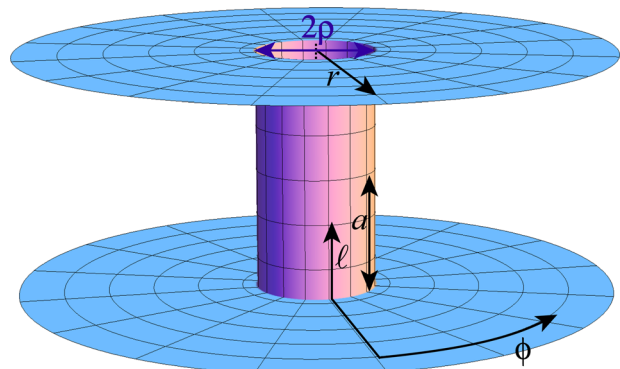


Fig. 2. Embedding diagram for the wormhole with sharp transition, Eqs. (1) and (3).

Somewhat arbitrarily, we chose to make the transition have approximately the same form as that from the throat (horizon) of a nonspinning black hole to the external universe in which the hole lives. Such a hole's metric (the “Schwarzschild metric”) has a form that is most simply written using radius  $r$  as the outward coordinate rather than proper distance  $\ell$ :

$$ds^2 = -(1 - 2\mathcal{M}/r)dt^2 + \frac{dr^2}{1 - 2\mathcal{M}/r} + r^2(d\theta^2 + \sin^2\theta d\phi^2), \quad (4)$$

where  $\mathcal{M}$  is the black hole's mass. Comparing the spatial part of this metric ( $t = \text{constant}$ ) with our general wormhole metric (1), we see that  $d\ell = \pm dr/\sqrt{1 - 2\mathcal{M}/r}$ , which can easily be integrated to obtain the proper distance traveled as a function of radius,  $\ell(r)$ . What we want, however, is  $r$  as a function of  $\ell$ , and we want it in an analytic form that is easy to work with. So for our Dneg wormhole, we choose a fairly simple analytic function that is roughly the same as the Schwarzschild  $r(\ell)$ .

Specifically, outside the wormhole's cylindrical interior, we chose

$$\begin{aligned} r &= \rho + \frac{2}{\pi} \int_0^{|\ell|-a} \arctan\left(\frac{2\xi}{\pi\mathcal{M}}\right) d\xi \\ &= \rho + \mathcal{M} \left[ x \arctan x - \frac{1}{2} \ln(1+x^2) \right], \quad \text{for } |\ell| > a, \end{aligned} \quad (5a)$$

where

$$x \equiv \frac{2(|\ell|-a)}{\pi\mathcal{M}}. \quad (5b)$$

(Students might want to compare this graphically with the inverse of the Schwarzschild  $\ell = \int dr/\sqrt{1 - 2\mathcal{M}/r}$ , plotting, e.g.,  $r - \rho$  for our wormhole as a function of  $|\ell| - a$ ; and  $r - 2M$  of Schwarzschild as a function of distance from the Schwarzschild horizon  $r = 2M$ .) Within the wormhole's cylindrical interior, we chose, of course,

$$r = \rho \quad \text{for } |\ell| < a. \quad (5c)$$

Equations (5) for  $r(\ell)$ , together with our general wormhole metric (1), describe the spacetime geometry of the Dneg wormhole without gravity.

For the Schwarzschild metric, the throat radius  $\rho$  is equal to twice the black hole's mass (in geometrized units),  $\rho = 2\mathcal{M}$ . For our Dneg wormhole, we choose the two parameters  $\rho$  and  $\mathcal{M}$  to be independent: they represent the wormhole's radius and the gentleness of the transition from the wormhole's cylindrical interior to its asymptotically flat exterior.

We shall refer to the ends of the cylindrical interior,  $\ell = \pm a$ , as the wormhole's *mouths*. They are spheres with circumferences  $2\pi\rho$ .

### 3. Embedding diagrams for the Dneg wormhole

We construct embedding diagrams for the Dneg wormhole (and any other spherical wormhole) by comparing the spatial

metric of the wormhole's two-dimensional equatorial surface  $ds^2 = d\ell^2 + r^2(\ell) d\phi^2$  with the spatial metric of the embedding space. Doing so is a good exercise for students. For the embedding space, we choose cylindrical coordinates with the symmetry axis along the wormhole's center line. Then (as in Figs. 1 and 2), the embedding space and the wormhole share the same radial coordinate  $r$  and angular coordinate  $\phi$ , so with  $z$  the embedding-space height above the wormhole's midplane, the embedding-space metric is  $ds^2 = dz^2 + dr^2 + r^2 d\phi^2$ . Equating this to the wormhole metric, we see that<sup>17</sup>  $dz^2 + dr^2 = d\ell^2$ , which gives us an equation for the height  $z$  of the wormhole surface as a function of distance  $\ell$  through the wormhole:

$$z(\ell) = \int_0^\ell \sqrt{1 - (dr/d\ell')^2} d\ell'. \quad (6)$$

By inserting the Dneg radius function (5) into this expression and performing the integral numerically, we obtain the wormhole shapes shown in Fig. 3 (and also Figs. 7 and 9).

The actual shape of this embedding diagram depends on two dimensionless ratios of the Dneg metric's three parameters: the wormhole's length-to-diameter ratio  $2a/2\rho = a/\rho$ , and its ratio  $\mathcal{M}/\rho$ . For chosen values of these ratios, the wormhole's size is then fixed by its interior radius  $\rho$ , which Christopher Nolan chose to be one kilometer in *Interstellar*, so with the technology of the movie's era the wormhole's gravitational lensing of our galaxy's star field can be seen from Earth, but barely so.<sup>18</sup>

In the embedding diagram of Fig. 3, instead of depicting  $\mathcal{M}$  we depict the lateral distance  $\mathcal{W}$  in the embedding space over which the wormhole's surface changes from vertical to 45 degrees. This  $\mathcal{W}$  is related to  $\mathcal{M}$  by<sup>19</sup>

$$\mathcal{W} = (1.42953\dots)\mathcal{M} \quad (7)$$

We call this  $\mathcal{W}$  the wormhole's *Lensing width*, and we often use it in place of  $\mathcal{M}$  as the wormhole's third parameter.

### 4. Dneg wormhole with gravity

Christopher Nolan asked for the movie's spacecraft Endurance to travel along a trajectory that gives enough time

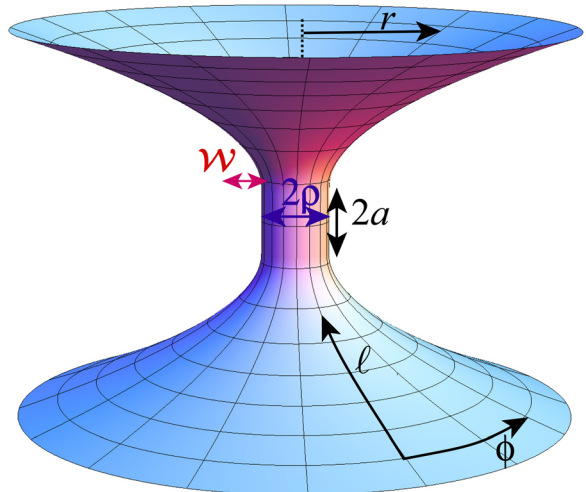


Fig. 3. Embedding diagram for the Dneg wormhole with parameters  $a/\rho = 1$  (length  $2a$  of cylindrical section equal to its diameter  $2\rho$ ) and  $\mathcal{M}/\rho = 0.5$ , which corresponds to a lensing width  $\mathcal{W}/\rho = 0.715$ .

for the audience to view the wormhole up close before Cooper, the pilot, initiates descent into the wormhole's mouth. Our Double Negative team designed such a trajectory, which required that the wormhole have a gravitational acceleration of order the Earth's,  $\sim 10 \text{ m/s}^2$ , or less. This is so weak that it can be described accurately by a Newtonian gravitational potential  $\Phi$  of magnitude  $|\Phi| \ll c^2 = 1$  (see below), that shows up in the time part of the metric. More specifically, we modify the wormhole's metric (1) to read

$$ds^2 = -(1 + 2\Phi)dt^2 + d\ell^2 + r^2(d\theta^2 + \sin^2\theta d\phi^2). \quad (8)$$

The sign of  $\Phi$  is negative (so the wormhole's gravity will be attractive), and spherical symmetry dictates that it be a function only of  $\ell$ .

According to the equivalence principle, the gravitational acceleration experienced by a particle at rest outside or inside the wormhole (at fixed spatial coordinates  $\{\ell, \theta, \phi\} = \text{constant}$ ) is the negative of that particle's 4-acceleration. Since the 4-acceleration is orthogonal to the particle's 4-velocity, which points in the time direction, its gravitational acceleration is purely spatial in the coordinate system  $\{t, \ell, \theta, \phi\}$ . It is a nice exercise for students to compute the particle's 4-acceleration and thence its gravitational acceleration. The result, aside from negligible fractional corrections of order  $|\Phi|$ , is

$$\mathbf{g} = -(d\Phi/d\ell) \mathbf{e}_\ell, \quad (9)$$

where  $\mathbf{e}_\ell$  is the unit vector pointing in the radial direction. Students may have seen an equation analogous to Eq. (8) when space is nearly flat, and a calculation in that case which yields Eq. (9) for  $\mathbf{g}$  (e.g., Sec. VI of Hartle<sup>11</sup>). Although for the wormhole metric (8), with  $r$  given by Eqs. (5) or (2), space is far from flat, Eq. (9) is still true—a deep fact that students would do well to absorb and generalize.

It is reasonable to choose the gravitational acceleration  $g = |\mathbf{g}| = |d\Phi/d\ell|$  to fall off as  $\sim 1/(\text{distance})^2$  as we move away from the wormhole mouth; or at least faster than  $\sim 1/(\text{distance})$ . Integrating  $g = |d\Phi/d\ell|$  radially and using this rapid falloff, the student can deduce that the magnitude of  $\Phi$  is of order  $g$  times the wormhole's radius  $\rho$ . With a gravitational acceleration  $g = |\mathbf{g}| \lesssim 10 \text{ m/s}^2$  and  $\rho = 1 \text{ km}$ , this gives  $|\Phi| \sim |\mathbf{g}|\rho \lesssim 10^4 (\text{m/s})^2 \sim 10^{-12}$ . Here, we have divided by the speed of light squared to bring this into our geometrized units.

Such a tiny gravitational potential corresponds to a slowing of time near the wormhole by the same small amount, no more than a part in  $10^{12}$  [cf. the time part of the metric (8)]. This is so small as to be utterly unimportant in the movie, and so small that, when computing the propagation of light rays through the wormhole, to ultrahigh accuracy we can ignore  $\Phi$  and use the Dneg metric without gravity. We shall do so.

### III. MAPPING A WORMHOLE'S TWO CELESTIAL SPHERES ONTO A CAMERA'S SKY

#### A. Foundations for the Map

A camera inside or near a wormhole receives light rays from light sources and uses them to create images. In this paper we shall assume, for simplicity, that all the light sources are far from the wormhole, so far that we can idealize them

as lying on “celestial spheres” at  $\ell \rightarrow -\infty$  (lower celestial sphere; Saturn side of the wormhole in the movie *Interstellar*) and  $\ell \rightarrow +\infty$  (upper celestial sphere; Gargantua side in *Interstellar*); see Fig. 4. (Gargantua is a supermassive black hole in the movie that humans visit.) Some light rays carry light from the lower celestial sphere to the camera's local sky (e.g., Ray 1 in Fig. 4); others carry light from the upper celestial sphere to the camera's local sky (e.g., Ray 2). Each of these rays is a null geodesic through the wormhole's spacetime.

On each celestial sphere we set up spherical polar coordinates  $\{\theta', \phi'\}$ , which are the limits of the spherical polar coordinates  $\{\theta, \phi\}$  as  $\ell \rightarrow \pm\infty$ . We draw these two celestial spheres in Fig. 5, a diagram of the three-dimensional space around each wormhole mouth, with the curvature of space not shown. Notice that we choose to draw the north polar axes  $\theta = 0$  pointing away from each other and the south polar axes  $\theta = \pi$  pointing toward each other. This is rather arbitrary, but it feels comfortable to us when we contemplate the embedding diagram of Fig. 4.

We assume the camera moves at speeds very low compared to light speed (as it does in *Interstellar*), so relativistic aberration and doppler shifts are unimportant. Therefore, when computing images the camera makes, we can treat the camera as at rest in the  $\{\ell, \theta, \phi\}$  coordinate system.

We can think of the camera as having a local sky on which there are spherical polar coordinates  $\{\theta_{\text{cs}}, \phi_{\text{cs}}\}$  (“cs” for camera sky; not to be confused with celestial sphere!); Fig. 5. In more technical language,  $\{\theta_{\text{cs}}, \phi_{\text{cs}}\}$  are spherical polar coordinates for the tangent space at the camera's location.

A light ray that heads backward in time from the camera (e.g., Ray 1 or 2 in Fig. 4), traveling in the  $\{\theta_{\text{cs}}, \phi_{\text{cs}}\}$  direction, ultimately winds up at location  $\{\theta', \phi'\}$  on one of the wormhole's two celestial spheres. It brings to  $\{\theta_{\text{cs}}, \phi_{\text{cs}}\}$  on the camera's sky an image of whatever was at  $\{\theta', \phi'\}$  on the celestial sphere.

This means that the key to making images of what the camera sees is a ray-induced map from the camera's sky to the celestial spheres:  $\{\theta', \phi', s\}$  as a function of  $\{\theta_{\text{cs}}, \phi_{\text{cs}}\}$ , where the parameter  $s$  tells us which celestial sphere the

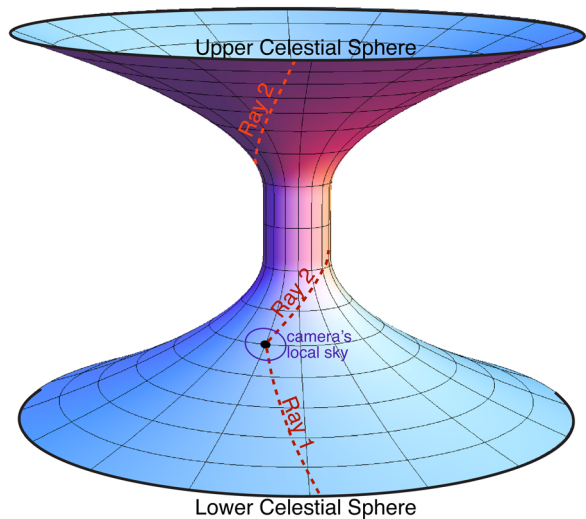


Fig. 4. Embedding diagram showing light rays 1 and 2 that carry light from a wormhole's lower and upper celestial spheres to a camera. The celestial spheres are incorrectly depicted close to the wormhole; they actually are very far away, and we idealize them as at  $\ell = \pm\infty$ .

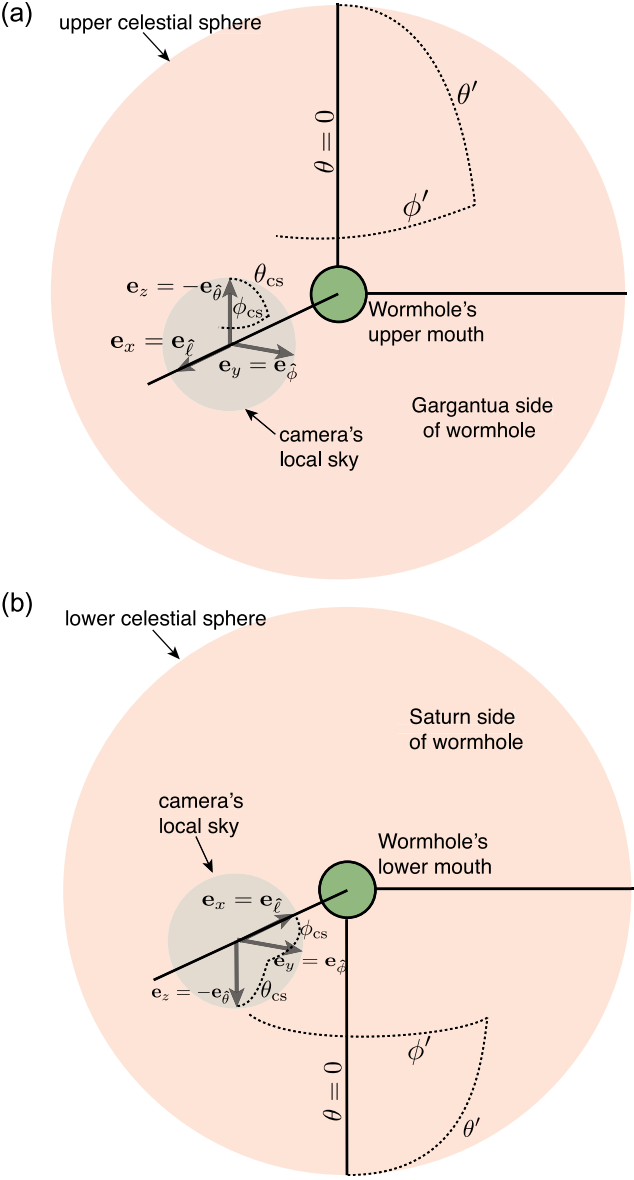


Fig. 5. The two sides of the wormhole, with a camera on each side at  $\theta_c = \pi/2$  (equatorial plane),  $\phi_c = 0$ , and  $\ell_c > a$  on the Gargantua side;  $\ell_c < -a$  on the Saturn side.

backward light ray reaches, the upper one ( $s = +$ ) or the lower one ( $s = -$ ).

In the Appendix, we sketch a rather simple computational procedure by which students can compute this map and then, using it, can construct images of wormholes and their surroundings. (We also describe a Mathematica implementation of this procedure by this paper's computationally challenged author Kip Thorne.)

## B. Our DNGR mapping and image making

To produce the IMAX images needed for *Interstellar*, at Double Negative we developed a much more sophisticated implementation of the map within a computer code that we call DNGR<sup>12</sup> (Double Negative Gravitational Renderer). In DNGR, we use ray bundles (light beams) to do the mapping rather than just light rays. We begin with a circular light beam about one pixel in size at the camera and trace it backward in time to its origin on a celestial sphere using the ray

equations (A7), plus the general relativistic equation of geodesic deviation, which evolves the beam's size and shape. At the celestial sphere, the beam is an ellipse, often highly eccentric. We integrate up the image data within that ellipse to deduce the light traveling into the camera's circular pixel. We also do spatial filtering to smooth artifacts and time filtering to mimic the behavior of a movie camera (when the image is changing rapidly), and we sometimes add lens flare to mimic the effects of light scattering and diffraction in a movie camera's lens.

Elsewhere<sup>12</sup> we give some details of these various "bells and whistles" for a camera orbiting a black hole rather than a wormhole. They are essentially the same for a wormhole.

However, fairly nice images can be produced without any of these bells and whistles, using the simple procedure described in the Appendix and thus are within easy reach of students in an elementary course on general relativity.

## IV. THE INFLUENCE OF THE WORMHOLE'S PARAMETERS ON WHAT THE CAMERA SEES

For Christopher Nolan's perusal in choosing *Interstellar*'s wormhole parameters, we used our map to make images of the galaxy in which the black hole Gargantua resides, as viewed from the Saturn side of the wormhole; see below. But for this paper, and the book<sup>5</sup> that Thorne has written about the science of *Interstellar*, we find it more instructive, pedagogically, to show images of Saturn and its rings as seen through the wormhole from the Gargantua side. This section is a more quantitative version of a discussion of this in Chapter 15 of that book.<sup>5</sup>

Figure 6 shows the simple Saturn image that we placed on the lower celestial sphere of Fig. 5, and a star field that we placed on the upper celestial sphere (the Gargantua side of the wormhole). Both images are mapped from the celestial sphere onto a flat rectangle with azimuthal angle  $\phi$  running horizontally and polar angle  $\theta$  vertically. In computer graphics, this type of image is known as a *longitude-latitude map*.<sup>21</sup>

### A. Influence of the Wormhole's length

In Fig. 7, we explore the influence of the wormhole's length on the camera-sky image produced by these two celestial spheres. Specifically, we hold the wormhole's lensing width fixed at a fairly small value,  $\mathcal{W} = 0.05\rho$ , and we vary the wormhole's length from  $2a = 0.01\rho$  (top picture), to  $2a = \rho$  (middle picture), to  $2a = 10\rho$  (bottom picture).

Because Saturn and its rings are white and the sky around it is black, while the star field on the Gargantua side of the wormhole is blue, we can easily identify the edge of the wormhole mouth as the transition from black-and-white to blue. (The light's colors are preserved as the light travels near and through the wormhole because we have assumed the wormhole's gravity is weak,  $|\Phi| \ll 1$ ; there are no significant gravitational frequency shifts.)

Through a short wormhole (top), the camera sees a large distorted image of Saturn nearly filling the right half of the wormhole mouth. This is the primary image, carried by light rays that travel on the shortest possible paths through the wormhole from Saturn to camera, such as path 1 in Fig. 8. There is also a very thin, lenticular, secondary image of Saturn, barely discernable, near the left edge of the wormhole mouth. It is brought to the camera by light rays that

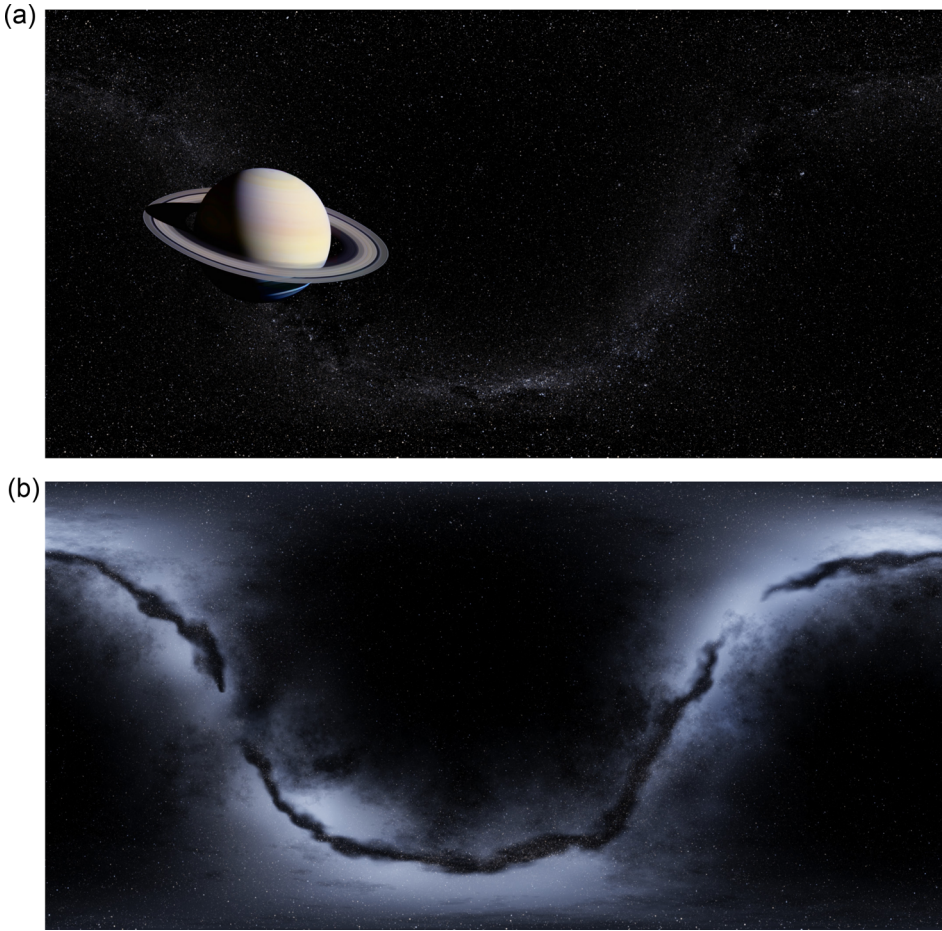


Fig. 6. (Top) The image of Saturn placed on the lower celestial sphere of Fig. 5 [from a composition of Cassini data by Mattias Malmer (Ref. 20)]. (Bottom) The star-field image placed on the upper celestial sphere (created by our Double Negative artistic team). These images are available in high resolution, for use by students, at <[http://www.dneg.com/dneg\\_vfx/wormhole](http://www.dneg.com/dneg_vfx/wormhole)>.

travel around the left side of the wormhole (e.g., path 2 in Fig. 8)—a longer route than for the primary image. The lenticular structure at the lower right is blue, so it is a secondary gravitationally lensed image of the blue star field that resides on the camera’s side of the wormhole.

As the wormhole is lengthened (middle of Fig. 7), the primary and secondary images move inward and shrink in size. A lenticular tertiary image emerges from the mouth’s right edge, carried by rays like 3 in Fig. 8 that wrap around the wormhole once; and a fourth (faint) lenticular image emerges from the left side, carried by rays like 4 that wrap around the wormhole in the opposite direction, one and a half times.

As the wormhole is lengthened more and more (bottom of Fig. 7), the existing images shrink and move inward toward the mouth’s center, and new images emerge, one after another, from the right then left then right... sides of the mouth.

For a short wormhole, all these images were already present, very near the wormhole’s edge; but they were so thin as to be unresolvable. Lengthening the wormhole moved them inward and made them thick enough to see.

## B. Influence of the Wormhole’s lensing width

In Fig. 9, we explore the influence of the wormhole’s lensing width on what the camera sees. We hold its length fixed and fairly small: equal to its radius,  $2a = \rho$ .

For small lensing width  $\mathcal{W} = 0.014\rho$  (top), the transition from the wormhole’s cylindrical interior to its asymptotically

flat exterior is quite sharp; so, not surprisingly, the camera sees an exterior, blue star field that extends with little distortion right up to the edge of the wormhole mouth.

By contrast, when the lensing width is larger,  $\mathcal{W} = 0.43\rho$  (bottom), the external star field is greatly distorted by gravitational lensing. The dark cloud on the upper left side of the wormhole is enlarged and pushed out of the cropped picture, and we see a big secondary image of the cloud on the wormhole’s lower right and a tertiary image on its upper left. We also see lensing of the wormhole mouth itself: it is enlarged; and lensing of the image that comes through the wormhole from the Saturn side. The lenticular secondary image of Saturn near the mouth’s left edge is thickened, while the primary image is shrunken a bit and moved inward to make room for a new tertiary image on the right.

Students could check their wormhole imaging code by trying to reproduce one or more images from Figs. 7 and 9, using the images in Fig. 6 on their celestial spheres. Having done so, they could further explore the influence of the wormhole parameters on the images the camera sees.

## V. INTERSTELLAR’S WORMHOLE

After reviewing images analogous to Figs. 7 and 9, but with Saturn replaced by the stars and nebulae of *Interstellar*’s distant galaxy (the galaxy on the Gargantua side of the wormhole), Christopher Nolan made his choice for the parameters of *Interstellar*’s wormhole.

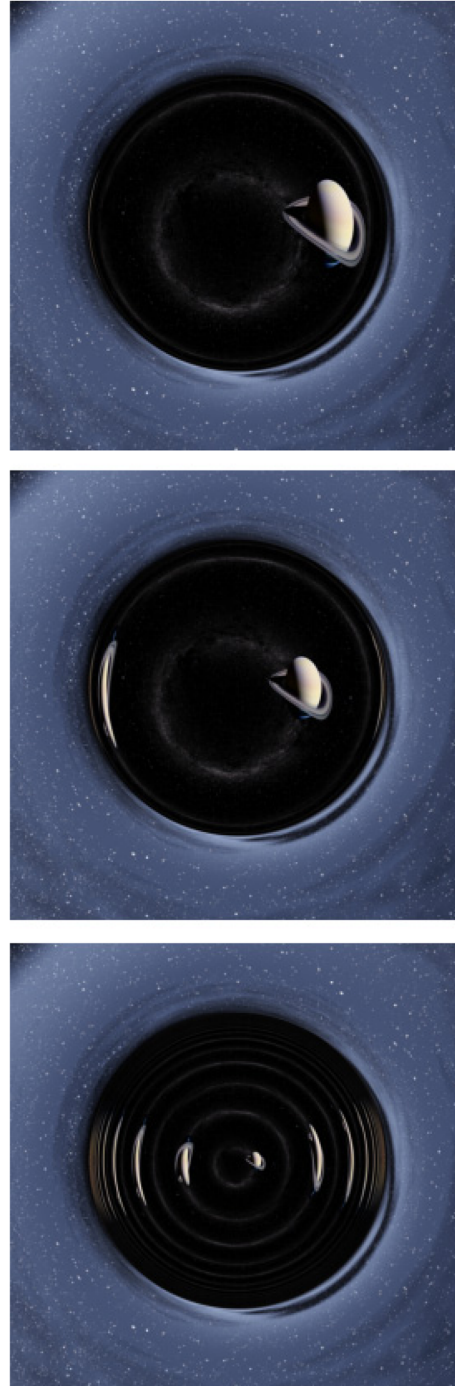
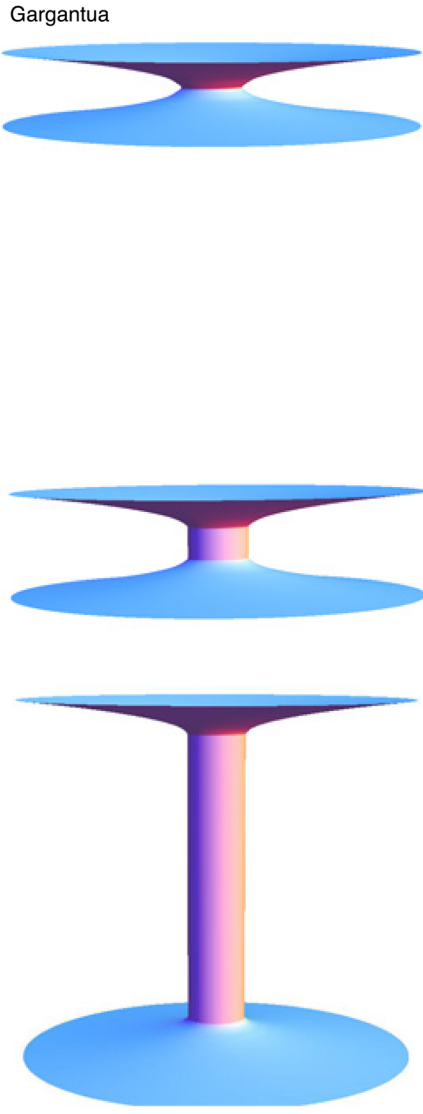


Fig. 7. Images of Saturn on the camera sky as seen through the wormhole, for small lensing width  $\mathcal{W} = 0.05\rho$  and various wormhole lengths (from top to bottom)  $2a/\rho = 0.01, 1, 10$ . The camera is at  $\ell = 6.25\rho + a$ ; i.e., at a distance  $6.25\rho$  from the wormhole’s mouth—the edge of its cylindrical interior. [Adapted from Fig. 15.2 of *The Science of Interstellar* (Ref. 5), and used by permission of W. W. Norton & Company, Inc. TM & Copyright 2015 Warner Bros. Entertainment Inc. (s15), and Kip Thorne. *Interstellar* and all related characters and elements are trademarks of and Copyright Warner Bros. Entertainment Inc. (s15). The images on the right may be used under the terms of the Creative Commons Attribution-NonCommercial-NoDerivs 3.0 (CC BY-NC-ND 3.0) license. Any further distribution of these images must maintain attribution to the author(s) and the title of the work, journal citation and DOI. You may not use the images for commercial purposes and if you remix, transform or build upon the images, you may not distribute the modified images.]

He chose a very short wormhole: length  $2a = 0.01\rho$  as in the top panel of Fig. 7; for greater lengths, the multiple images would be confusing to a mass audience. And he chose a modest lensing width:  $\mathcal{W} = 0.05\rho$  also as in the top panel of Fig. 7 and in between the two lensing widths of Fig. 9. This gives enough gravitational lensing to be interesting (see below), but far less lensing than for a black hole, thereby

enhancing the visual distinction between *Interstellar*’s wormhole and its black hole Gargantua.

#### A. *Interstellar*’s distant galaxy

For *Interstellar*, a team under the leadership of authors Paul Franklin and Eugénie von Tunzelmann constructed images of the distant galaxy through a multistep process.

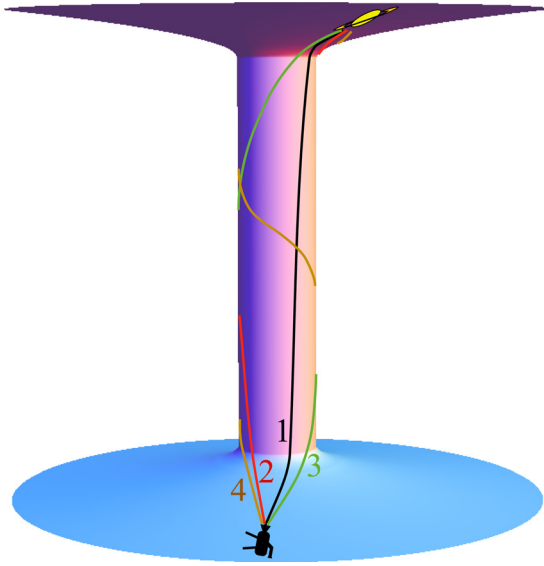


Fig. 8. Light rays that travel from Saturn, though the Dneg wormhole, to the camera, producing the images in Fig. 7. [Adapted from Fig. 15.3 of *The Science of Interstellar* (Ref. 5).]

The distant end of the wormhole was imagined to be in the distant galaxy and closer to its center than we are to the center of our Milky Way. Consequently, the view of the

surrounding galaxy must be recognisably different from the view we have from Earth: larger and brighter nebulae, more dense dust, with brighter and more numerous visible stars. This view was created as an artistic task.

Nebulae were painted (by texture artist Zoe Lord), using a combination of space photography and imagination, covering a range of color palettes. These were combined with layers of painted bright space dust and dark, silhouetted dust channels, to create a view of the galaxy with as much visual depth and complexity as possible.

Star layout was achieved by taking real star data as seen from Earth and performing various actions to make the view different: the brightest stars were removed from the data set (to avoid recognisable constellations) and the brightnesses of all the other stars were increased and shuffled. The result was a believably natural-looking star layout which was unrecognisable compared to our familiar view of the night sky from Earth.

Figure 10 is one of our distant-galaxy images, showing nebulae, space dust, and stars.

## B. View through *Interstellar's* Wormhole

When we place this distant-galaxy image on the upper celestial sphere of Fig. 5 and place a simple star field on the lower celestial sphere, within which the camera resides, then

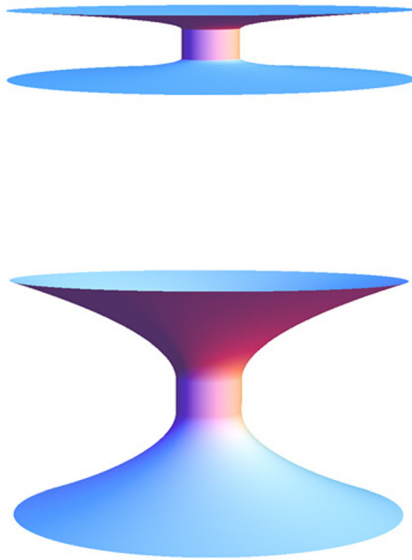


Fig. 9. Images of Saturn on the camera sky, as seen through a wormhole with fixed length equal to the wormhole radius,  $2a = \rho$ , and for two lensing widths:  $\mathcal{W} = 0.014\rho$  (top) and  $\mathcal{W} = 0.43$  (bottom). [Adapted from Fig. 15.4 of *The Science of Interstellar* (Ref. 5), and used by permission of W. W. Norton & Company, Inc. TM & Copyright Warner Bros. Entertainment Inc. (s15), and Kip Thorne. The images on the right may be used under the terms of the Creative Commons Attribution-NonCommercial-NoDerivs 3.0 (CC BY-NC-ND 3.0) license. Any further distribution of these images must maintain attribution to the author(s) and the title of the work, journal citation and DOI. You may not use the images for commercial purposes and if you remix, transform or build upon the images, you may not distribute the modified images.]

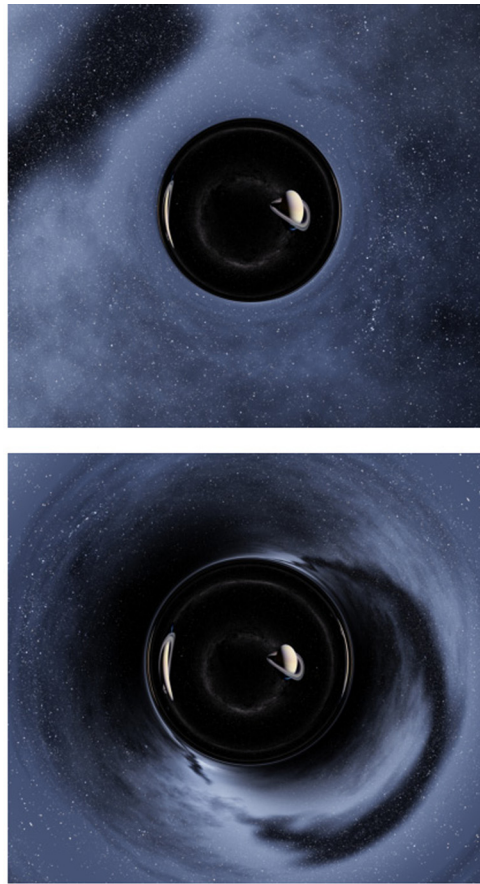




Fig. 10. An image of stars and nebulae in *Interstellar*'s distant galaxy (the galaxy on the Gargantua side of the wormhole), created by our Double Negative artistic team. This image is available in high resolution, for use by students, at <[http://www.dneg.com/dneg\\_vfx/wormhole](http://www.dneg.com/dneg_vfx/wormhole)>.

the moving camera sees the wormhole images shown in *Interstellar* and its trailers; for example, Fig. 11.

Students can create similar images, using their implementation of the map described in the Appendix, and putting Fig. 10 on the upper celestial sphere. They could be invited to explore how their images change as the camera moves farther from the wormhole, closer, and through it, and as the wormhole parameters are changed.

### C. The Einstein ring

Students could be encouraged to examine closely the changing image of the wormhole in *Interstellar* or one of its trailers, on a computer screen where the student can move

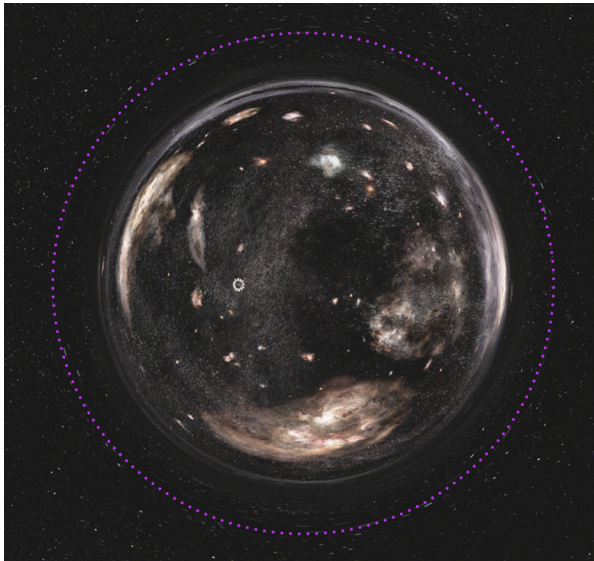


Fig. 11. An image of the distant galaxy seen through *Interstellar*'s wormhole. The dotted pink circle is the wormhole's Einstein ring. [From a trailer for *Interstellar*. Created by our Double Negative team. TM & Copyright Warner Bros. Entertainment Inc. (s15). This image may be used under the terms of the Creative Commons Attribution-NonCommercial-NoDerivs 3.0 (CC BY-NC-ND 3.0) license. Any further distribution of these images must maintain attribution to the author(s) and the title of the work, journal citation and DOI. You may not use the images for commercial purposes and if you remix, transform or build upon the images, you may not distribute the modified images.]

the image back and forth in slow motion. Just outside the wormhole's edge, at the location marked by a dotted circle in Fig. 11, the star motions (induced by camera movement) are quite peculiar. On one side of the dotted circle, stars move rightward; on the other, leftward. The closer a star is to the circle, the faster it moves; see Fig. 12.

The circle is called the wormhole's *Einstein ring*. This ring is actually the ring image, on the camera's local sky, of a tiny light source that is precisely behind the wormhole and on the same end of the wormhole as the camera. That

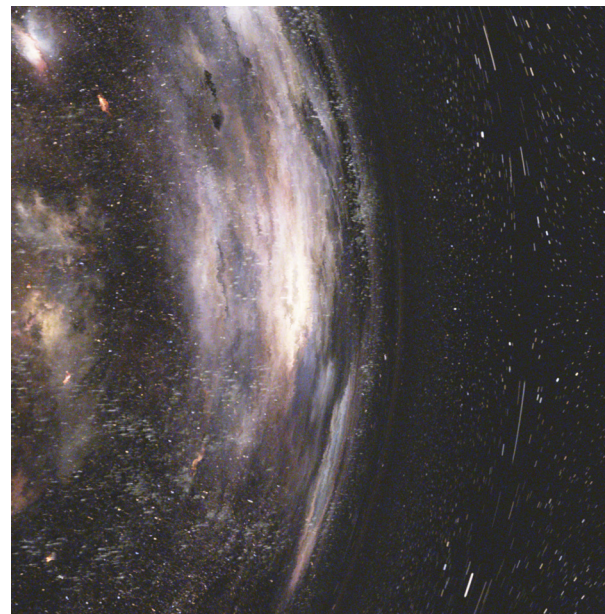


Fig. 12. A close-up of *Interstellar*'s wormhole. The long, streaked stars alongside the *Einstein ring* are a result of motion blur: the virtual camera's shutter is open for a fraction of a second (in this case, approximately 0.02 s) during which the stars' lensed images appear to orbit the wormhole, causing the curved paths seen here. [From *Interstellar*, but cropped. Created by our Double Negative team. TM & Copyright Warner Bros. Entertainment Inc. (s15). This image may be used under the terms of the Creative Commons Attribution-NonCommercial-NoDerivs 3.0 (CC BY-NC-ND 3.0) license. Any further distribution of these images must maintain attribution to the author(s) and the title of the work, journal citation and DOI. You may not use the images for commercial purposes and if you remix, transform or build upon the images, you may not distribute the modified images.]

location, on the celestial sphere and precisely opposite the camera, is actually a *caustic* (a singular, focal point) of the camera's past light cone. As the camera orbits the wormhole, causing this caustic to sweep very close to a star, the camera sees two images of the star, one just inside the Einstein ring and the other just outside it, move rapidly around the ring in opposite directions. This is the same behavior as occurs with the Einstein ring of a black hole (see, e.g., Fig. 2 of our paper on black-hole lensing<sup>12</sup>) and any other spherical gravitational lens, and it is also responsible for long, lenticular images of distant galaxies gravitationally lensed by a more nearby galaxy.<sup>22</sup>

Students, having explored the wormhole's Einstein ring in a DVD or trailer of the movie, could be encouraged to go learn about Einstein rings and/or figure out for themselves how these peculiar star motions are produced. They could then use their own implementation of our map to explore whether their explanation is correct.

## VI. TRIP THROUGH THE WORMHOLE

Students who have implemented the map (described in the Appendix) from the camera's local sky to the celestial spheres could be encouraged to explore, with their implementation, what it looks like to travel through the Dneg wormhole for various parameter values.

We ourselves did so, together with Christopher Nolan, as a foundation for *Interstellar*'s wormhole trip. Because the wormhole Nolan chose to visualize from the outside (upper left of Fig. 7; images in Figs. 10 and 12) is so short and its

lensing width so modest, the trip was quick and not terribly interesting, visually—not at all what Nolan wanted for his movie. So we generated additional through-the-wormhole clips for him, with the wormhole parameters changed. For a long wormhole, the trip was like traveling through a long tunnel, too much like things seen in previous movies. None of the clips, for any choice of parameters, had the compelling freshness that Nolan sought.

Moreover, none had the right *feel*. Figure 13 illustrates this problem. This figure shows stills from a trip through a moderately short wormhole with  $a/\rho = 0.5$  (stills that students could replicate with their implementation). Although these images are interesting, the resulting animated sequence is hard for an audience to interpret. The view of the wormhole appears to scale up from its center, growing in size until it fills the frame, and until none of the starting galaxy is visible; at this point only the new galaxy can be seen, because we now are actually inside that new galaxy. This is hard to interpret visually. Because there is no parallax or other relative motion in the frame, to the audience it looks like the camera is zooming into the center of the wormhole using the camera's zoom lens. In the visual grammar of filmmaking, this tells the audience that we are zooming in for a closer look but we are still a distance from the wormhole; in reality we are travelling through it, but this is not how it feels.

It was important for the audience to understand that the wormhole allows the Endurance (the movie's space ship) to take a shortcut through the higher dimensional bulk. To foster that understanding, Nolan asked the visual effects team to convey a sense of travel through an exotic environment, one

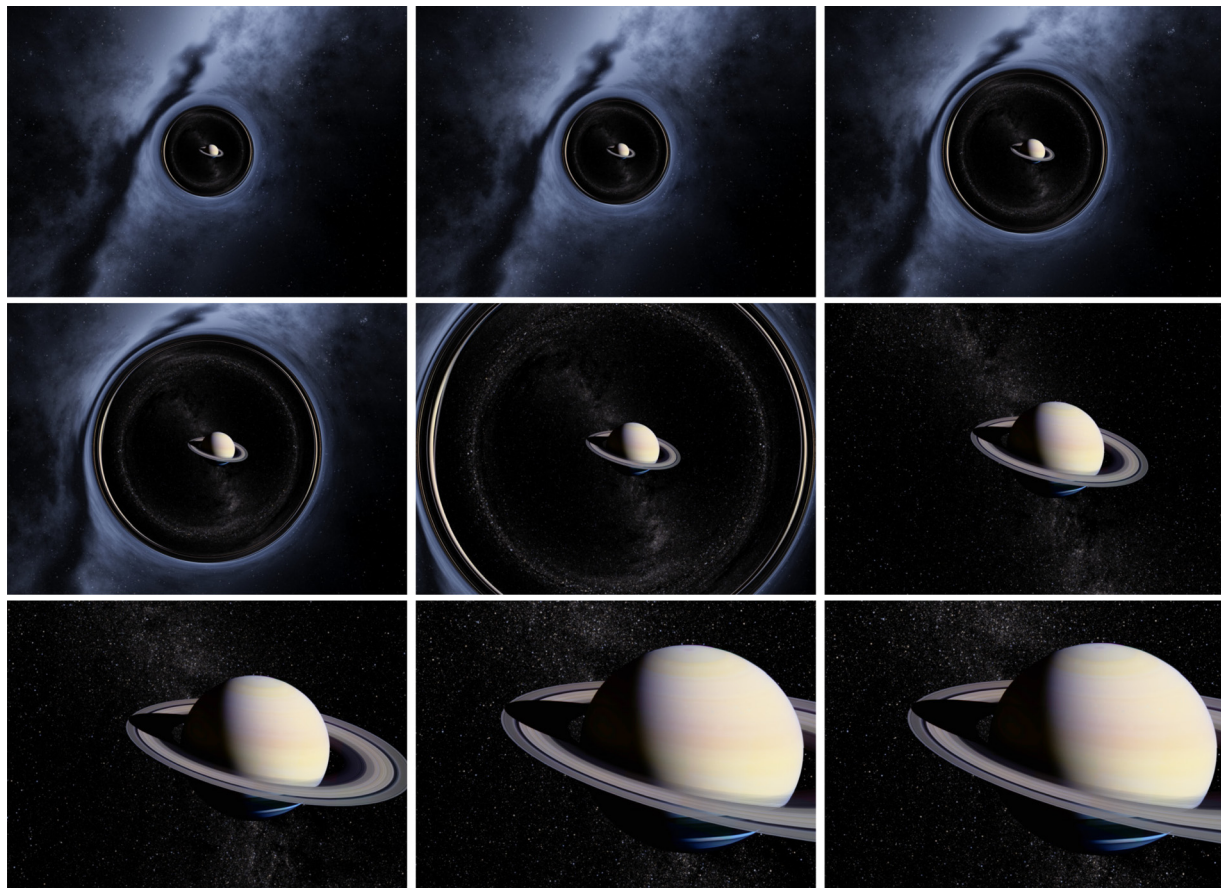


Fig. 13. Still frames of a voyage through a short wormhole ( $a/\rho = 0.5$ ) with weak lensing ( $\mathcal{W}/\rho = 0.05$ ), as computed with our DNGR code.

that was thematically linked to the exterior appearance of the wormhole but also incorporated elements of passing landscapes and the sense of a rapidly approaching destination. The visual effects artists at Double Negative combined existing DNGR visualisations of the wormhole's interior with layers of interpretive effects animation derived from aerial photography of dramatic landscapes, adding lens-based photographic effects to tie everything in with the rest of the sequence. The end result was a sequence of shots that told a story comprehensible by a general audience while resembling the wormhole's interior, as simulated with DNGR.

## VII. CONCLUSION

As we wrote this paper, we became more and more enthusiastic about the educational opportunities provided by our *Interstellar* experience. The tools we used in building, scoping out, and exploring *Interstellar*'s wormhole—at least those discussed in this paper—should be easily accessible to fourth year undergraduates studying relativity, as well as to graduate students. And the movie itself, and our own route to the final wormhole images in the movie, may be a strong motivator for students.

## ACKNOWLEDGMENTS

For extensive advice on our wormhole visualizations, the authors thank Christopher Nolan. For contributions to DNGR and its wormhole applications, the authors thank members of the Double Negative R&D team Sylvan Dieckmann, Simon Pabst, Shane Christopher, Paul-George Roberts, and Damien Maupu; and also Double Negative artists Zoe Lord, Fabio Zangla, Iacopo di Luigi, Finella Fan, Tristan Myles, Stephen Tew, and Peter Howlett. The construction of our code DNGR was funded by Warner Bros. Entertainment Inc., for generating visual effects for the movie *Interstellar*. The authors thank Warner Bros. for authorizing this code's additional use for scientific research and physics education, and in particular the work reported in this paper.

## APPENDIX: THE RAY-INDUCED MAP FROM THE CAMERA'S LOCAL SKY TO THE TWO CELESTIAL SPHERES

In this Appendix, we describe our fairly simple procedure for generating the map from points  $\{\theta_{\text{cs}}, \phi_{\text{cs}}\}$  on the camera's local sky to points  $\{\theta', \phi', s\}$  on the wormhole's celestial sphere, with  $s = +$  for the upper celestial sphere and  $s = -$  for the lower.

### 1. The ray equations

As we discussed in Sec. III A, the map is generated by light rays that travel backward in time from the camera to the celestial spheres. In the language of general relativity, these light rays are null (light-like) geodesics and so are solutions of the geodesic equation

$$\frac{d^2x^\alpha}{d\zeta^2} + \Gamma^\alpha_{\mu\nu} \frac{dx^\mu}{d\zeta} \frac{dx^\nu}{d\zeta} = 0. \quad (\text{A1})$$

Here, the  $\Gamma^\alpha_{\mu\nu}$  are Christoffel symbols (also called connection coefficients) that are constructable from first derivatives

of the metric coefficients, and  $\zeta$  is the so-called *affine parameter*, which varies along the geodesic.

This form of the geodesic equation is fine for analytical work, but for numerical work, it is best rewritten in the language of Hamiltonian mechanics. Elsewhere<sup>23</sup> one of us will discuss, pedagogically, the advantages and the underpinnings of this Hamiltonian rewrite.

There are several different Hamiltonian formulations of the geodesic equation. The one we advocate is sometimes called the “super-Hamiltonian” because of its beauty and power, but we will stick to the usual word “Hamiltonian.” The general formula for this Hamiltonian is<sup>23,24</sup>

$$H(x^\alpha, p_\beta) = \frac{1}{2} g^{\mu\nu}(x^\alpha) p_\mu p_\nu. \quad (\text{A2})$$

Here,  $g^{\mu\nu}$  are the contravariant components of the metric,  $x^\alpha$  is the coordinate of a photon traveling along the ray, and  $p_\alpha$  is the generalized momentum that is canonically conjugate to  $x^\alpha$ , which turns out to be the same as the covariant component of the photon's 4-momentum. Hamilton's equations, with the affine parameter  $\zeta$  playing the role of time, take the standard form

$$\frac{dx^\alpha}{d\zeta} = \frac{\partial H}{\partial p_\alpha} = g^{\alpha\nu} p_\nu, \quad (\text{A3a})$$

$$\frac{dp_\alpha}{d\zeta} = -\frac{\partial H}{\partial x^\alpha} = -\frac{1}{2} \frac{\partial g^{\mu\nu}}{\partial x^\alpha} p_\mu p_\nu. \quad (\text{A3b})$$

In the first of Eqs. (A3), the metric raises the index on the covariant momentum, so it becomes  $p^\alpha = dx^\alpha/d\zeta$ , an expression that may be familiar to students. The second expression may not be so familiar, but it can be given as an exercise for students to show that the second equation, together with  $p^\alpha = dx^\alpha/d\zeta$ , is equivalent to the usual form (A1) of the geodesic equation.

For the general wormhole metric (1), the (super) Hamiltonian (A2) has the simple form

$$H = \frac{1}{2} \left[ -p_t^2 + p_\ell^2 + \frac{p_\theta^2}{r(\ell)^2} + \frac{p_\phi^2}{r(\ell)^2 \sin^2 \theta} \right]. \quad (\text{A4})$$

Because this (super) Hamiltonian is independent of the time coordinate  $t$  and of the azimuthal coordinate  $\phi$ ,  $p_t$  and  $p_\phi$  are conserved along a ray [cf. Eq. (A3b)]. Since  $p^t = dt/d\zeta = -p_t$ , changing the numerical value of  $p_t$  merely renormalizes the affine parameter  $\zeta$ ; so without loss of generality, we set  $p_t = -1$ , which implies that  $\zeta$  is equal to time  $t$  [Eq. (A6)]. Since photons travel at the speed of light,  $\zeta$  is also distance travelled (in our geometrized units where the speed of light is one).

We use the notation  $b$  for the conserved quantity  $p_\phi$ :

$$b = p_\phi. \quad (\text{A5a})$$

Students should easily be able to show that, because we set  $p_t = -1$ , this  $b$  is the ray's impact parameter relative to the (arbitrarily chosen<sup>25</sup>) polar axis. Because the wormhole is spherical, there is a third conserved quantity for the rays, its total angular momentum, which (with  $p_t = -1$ ) is the same as its impact parameter  $B$  relative to the hole's center

$$B^2 = p_\theta^2 + \frac{p_\phi^2}{\sin^2 \theta}. \quad (\text{A5b})$$

By evaluating Hamilton's equations for the wormhole Hamiltonian (A4) and inserting the conserved quantities on the right-hand side, we obtain the following ray equations:

$$\frac{dt}{d\zeta} = -p_t = 1, \quad (\text{A6})$$

which reaffirms that  $\zeta = t$  (up to an additive constant); and, replacing  $\zeta$  by  $t$ :

$$\frac{d\ell}{dt} = p_\ell, \quad (\text{A7a})$$

$$\frac{d\theta}{dt} = \frac{p_\theta}{r^2}, \quad (\text{A7b})$$

$$\frac{d\phi}{dt} = \frac{b}{r^2 \sin^2 \theta}, \quad (\text{A7c})$$

$$\frac{dp_\ell}{dt} = B^2 \frac{dr/d\ell}{r^3}, \quad (\text{A7d})$$

$$\frac{dp_\theta}{dt} = \frac{b^2 \cos \theta}{r^2 \sin^3 \theta}. \quad (\text{A7e})$$

These are five equations for the five quantities  $\{\ell, \theta, \phi, p_\ell, p_\theta\}$  as functions of  $t$  along the geodesic (ray). It is not at all obvious from these equations, but they guarantee (in view of spherical symmetry) that the lateral (nonradial) part of each ray's motion is along a great circle.

These equations may seem like an overly complicated way to describe a ray. Complicated, maybe, but near ideal for simple numerical integrations. They are stable and in all respects well behaved everywhere except the poles  $\theta=0$  and  $\theta=\pi$ , and they are easily implemented in student-friendly software such as Mathematica, Maple, and Matlab.

## 2. Procedure for generating the map

It is an instructive exercise for students to verify the following procedure for constructing the map from the camera's local sky to the two celestial spheres:

- (1) Choose a camera location  $(\ell_c, \theta_c, \phi_c)$ . It might best be on the equatorial plane,  $\theta_c = \pi/2$ , so the coordinate singularities at  $\theta=0$  and  $\theta=\pi$  are as far from the camera as possible.
- (2) Set up local Cartesian coordinates centered on the camera, with  $x$  along the direction of increasing  $\ell$  (toward the wormhole on the Saturn side; away from the wormhole on the Gargantua side),  $y$  along the direction of increasing  $\phi$ , and  $z$  along the direction of *decreasing*  $\theta$ ,

$$\mathbf{e}_x = \mathbf{e}_\ell, \quad \mathbf{e}_y = \mathbf{e}_\phi, \quad \mathbf{e}_z = -\mathbf{e}_\theta. \quad (\text{A8})$$

Here  $\mathbf{e}_\ell$ ,  $\mathbf{e}_\theta$ , and  $\mathbf{e}_\phi$  are unit vectors that point in the  $\ell$ ,  $\theta$ , and  $\phi$  directions (the hats tell us their lengths are one). Figure 5 shows these camera basis vectors for the special case where the camera is in the equatorial plane. The minus sign in our choice  $\mathbf{e}_z = -\mathbf{e}_\theta$  makes the camera's  $\mathbf{e}_z$  parallel to the wormhole's polar axis on the Gargantua side of the wormhole, where  $\ell$  is positive.

- (3) Set up a local spherical polar coordinate system for the camera's local sky in the usual way, based on the camera's local Cartesian coordinates; cf. Eq. (A9a).

- (4) Choose a direction  $(\theta_{cs}, \phi_{cs})$  on the camera's local sky. The unit vector  $\mathbf{N}$  pointing in that direction has Cartesian components

$$\begin{aligned} N_x &= \sin \theta_{cs} \cos \phi_{cs}, & N_y &= \sin \theta_{cs} \sin \phi_{cs}, \\ N_z &= \cos \theta_{cs}. \end{aligned} \quad (\text{A9a})$$

Because of the relationship (A8) between bases, the direction  $\mathbf{n}$  of propagation of the incoming ray that arrives from direction  $-\mathbf{N}$  has components in the global spherical polar basis

$$n_{\hat{\ell}} = -N_x, \quad n_{\hat{\phi}} = -N_y, \quad n_{\hat{\theta}} = +N_z. \quad (\text{A9b})$$

- (5) Compute the incoming light ray's canonical momenta from

$$p_\ell = n_{\hat{\ell}}, \quad p_\theta = r n_{\hat{\theta}}, \quad p_\phi = r \sin \theta n_{\hat{\phi}} \quad (\text{A9c})$$

(it's a nice exercise for students to deduce these equations from the relationship between the covariant components of the photon 4-momentum and the components on the unit basis vectors). Then compute the ray's constants of motion from

$$\begin{aligned} b &= p_\phi = r \sin \theta n_{\hat{\phi}}, \\ B^2 &= p_\theta^2 + \frac{p_\phi^2}{\sin^2 \theta} = r^2 \left( n_{\hat{\theta}}^2 + n_{\hat{\phi}}^2 \right). \end{aligned} \quad (\text{A9d})$$

- (6) Take as initial conditions for ray integration that at  $t=0$  the ray begins at the camera's location  $(\ell, \theta, \phi) = (\ell_c, \theta_c, \phi_c)$  with canonical momenta (A9c) and constants of motion (A9d). Numerically integrate the ray equations (A7), subject to these initial conditions, from  $t=0$  backward along the ray to time  $t_i = -\infty$  (or some extremely negative, finite initial time  $t_i$ ). If  $\ell(t_i)$  is negative, then the ray comes from location  $\{\theta', \phi'\} = \{\theta(t_i), \phi(t_i)\}$  on the Saturn side of the wormhole,  $s=-$ . If  $\ell(t_i)$  is positive, then the ray comes from location  $\{\theta', \phi'\} = \{\theta(t_i), \phi(t_i)\}$  on the Gargantua side of the wormhole,  $s=+$ .

## 3. Implementing the map

Evaluating this map numerically should be a moderately easy task for students. Kip Thorne, the author among us who is least adept at numerical work, did it using Mathematica, and then used that map—a numerical table of  $\{\theta', \phi', s\}$  as a function of  $\{\theta_{cs}, \phi_{cs}\}$ —to make camera-sky images of whatever was placed on the two celestial spheres. For image processing, Thorne first built an interpolation of the map using the Mathematica command `ListInterpolation`; and he then used this interpolated map, together with Mathematica's command `ImageTransformation`, to produce the camera-sky image from the images on the two celestial spheres.

<sup>1</sup>Carl Sagan, *Contact* (Simon and Schuster, New York, 1985).

<sup>2</sup>*Contact*, The Movie, directed by Robert Zemeckis (© Warner Bros., 1997).

<sup>3</sup>Michael S. Morris and Kip S. Thorne, "Wormholes in spacetime and their use for interstellar travel: A tool for teaching general relativity," *Am. J. Phys.* **56**, 395–412 (1988).

- <sup>4</sup>*Interstellar*, directed by Christopher Nolan, screenplay by Jonathan Nolan and Christopher Nolan (© Warner Bros, 2014).
- <sup>5</sup>Kip Thorne, *The Science of Interstellar* (W.W. Norton and Company, New York, 2014).
- <sup>6</sup>Allen Everett and Thomas Roman, *Time Travel and Warp Drives* (University of Chicago Press, Chicago, 2012).
- <sup>7</sup>John L. Friedman and Atsushi Higuchi “Topological censorship and chronology protection,” *Ann. Phys.* **15**, 109–128 (2006).
- <sup>8</sup>Francisco S. N. Lobo “Exotic solutions in general relativity: Traversable wormholes and ‘warp drive’ spacetimes,” *Classical and Quantum Gravity Research 5 Progress* (Nova Science Publishers, Hauppauge, NY, 2008), pp. 1–78.
- <sup>9</sup>Michael S. Morris, Kip S. Thorne, and Ulvi Yurtsever, “Wormholes, time machines, and the weak energy condition,” *Phys. Rev. Lett.* **61**, 1446–1449 (1988).
- <sup>10</sup>See, e.g., chapter 13 of *The Science of Interstellar*<sup>4</sup>.
- <sup>11</sup>James B. Hartle, *Gravity: An Introduction to Einstein’s General Relativity* (Addison-Wesley, San Francisco, 2003).
- <sup>12</sup>Oliver James, Eugénie von Tunzelmann, Paul Franklin, and Kip S. Thorne, “Gravitational lensing by spinning black holes in astrophysics, and in the movie *Interstellar*,” *Class. Quant. Grav.* **32**, 065001 (2015).
- <sup>13</sup>Homer G. Ellis, “Ether flow through a drainhole: A particle model in general relativity,” *J. Math. Phys.* **14**, 104–118 (1973).
- <sup>14</sup>Fifteen years later, Morris and Thorne<sup>3</sup> wrote down this same metric, among others, and being unaware of Ellis’s paper, failed to attribute it to him, for which they apologize. Regretably, it is sometimes called the Morris-Thorne wormhole metric.
- <sup>15</sup>Thomas Müller, “Visual appearance of a Morris-Thorne-Wormhole,” *Am. J. Phys.* **72**, 1045–1050 (2004), which is based in part on Daniel Weiskopf, “Visualization of four-dimensional spacetimes,” Ph.D thesis at der Eberhard-Karls-Universität zu Tübingen, available at <http://nbn-resolving.de/urn:nbn:de:bsz:21-opus-2400>.
- Wormhole images based on Müller’s paper are available at [https://www.youtube.com/watch?v=FHmupoY4nZU&index=2&list=PLdclGldT8\\_FEnv0MmGrb04azONGpgqbq7](https://www.youtube.com/watch?v=FHmupoY4nZU&index=2&list=PLdclGldT8_FEnv0MmGrb04azONGpgqbq7), and also in the paper Hans Ruder *et al.*, “How computers can help us in creating an intuitive access to relativity,” *New J. Phys.* **10**, 125014 (2008). For a movie by Covin Zahn of what it looks like to travel through an Ellis wormhole, see <http://www.spacetimetravel.org/wurmlochflug/wurmlochflug.html>.
- <sup>16</sup>Tomaso Treu, Philip J. Marshall, and Douglas Clowe, “Resource Letter GL-1: Gravitational Lensing,” *Am. J. Phys.* **80**, 753–763 (2012); <http://arxiv.org/pdf/1206.0791v1.pdf> and <https://groups.diigo.com/group/gravitational-lensing>.
- <sup>17</sup>This is the same as Eq. (7.46b) of Hartle,<sup>11</sup> where, however, our  $\ell$  is denoted  $\rho$ .
- <sup>18</sup>See the technical notes for chapter 15 of *The Science of Interstellar*,<sup>5</sup> pp. 294–295.
- <sup>19</sup>From the embedding equation (6) and  $dr/d\ell = (2/\pi)\arctan(2\ell/\pi\mathcal{M})$  [Eq. (5b)], it follows that  $\mathcal{W}/\mathcal{M} = -\ln[\sec(\pi/2\sqrt{2})] + (\pi/2\sqrt{2})\tan(\pi/2\sqrt{2}) = 1.42053\dots$
- <sup>20</sup>Mattias Malmer, <http://apod.nasa.gov/apod/ap041225.html>.
- <sup>21</sup>J. F. Blinn and M. E. Newell, “Texture and reflection in computer generated images,” *Commun. ACM* **19**, 542–547 (1976).
- <sup>22</sup>M. Bartelmann “Gravitational lensing,” *Class. Quant. Grav.* **27**, 233001 (2010).
- <sup>23</sup>Richard H. Price and Kip S. Thorne, “Superhamiltonian for geodesic motion and its power in numerical computations,” *Am. J. Phys.* (in preparation).
- <sup>24</sup>Charles W. Misner, Kip S. Thorne, and John Archibald Wheeler, *Gravitation* (W. H. Freeman, San Francisco, 1973).
- <sup>25</sup>The polar axis is arbitrary because the wormhole’s geometry is spherically symmetric.



**Rowland’s Ring**

Rowland’s Ring is a device for tracing out curves of magnetic induction,  $\mathbf{B}$ , as a function of the magnetizing field,  $\mathbf{H}$ , for an iron ring. These curves are called Hysteresis Curves. There are two coils wound on the ring: a coil that delivers a short pulse of current to create the  $\mathbf{H}$  field, and a pickup coil in which the EMF produced by the resulting  $\mathbf{B}$  field is detected. Today it would be easy to design circuits using op amp integrating circuits to do the experiment; in my academic childhood we used wall galvanometers with coils with large moments of inertia to detect the secondary current. It was developed by Henry Augustus Rowland (1848–1901). This example is in the Greenslade Collection. (Notes and photograph by Thomas B. Greenslade, Jr., Kenyon College)